ELSEVIER

Chemical Geology 188 (2002) 65–83

CHEMICAL GEOLOGY
INCLUDING
ISOTOPE GEOSCIENCE

www.elsevier.com/locate/chemgeo

Applications of accurate, high-precision Pb isotope ratio measurement by multi-collector ICP-MS

Kenneth D. Collerson *, Balz S. Kamber, Ronny Schoenberg

Department of Earth Sciences, Advanced Centre for Queensland University Isotope Research Excellence (ACQUIRE), The University of Queensland, Steele Building, St. Lucia, Brisbane, QLD 4072, Australia

Received 17 May 2001; accepted 2 April 2002

Abstract

The isotope composition of Pb is difficult to determine accurately due to the lack of a stable normalisation ratio. Double and triple-spike addition techniques provide one solution and presently yield the most accurate measurements. A number of recent studies have claimed that improved accuracy and precision could also be achieved by multi-collector ICP-MS (MC-ICP-MS) Pb-isotope analysis using the addition of Tl of known isotope composition to Pb samples. In this paper, we verify whether the known isotope composition of Tl can be used for correction of mass discrimination of Pb with an extensive dataset for the NIST standard SRM 981, comparison of MC-ICP-MS with TIMS data, and comparison with three isochrons from different geological environments.When all our NIST SRM 981 data are normalised with one constant $^{205}Tl/^{203}Tl$ of 2.38869, the following averages and reproducibilities were obtained: $^{207}Pb/^{206}Pb = 0.91461 \pm 18$; $^{208}Pb/^{206}Pb = 2.1674 \pm 7$; and $^{206}Pb/^{204}Pb = 16.941 \pm 6$. These two sigma standard deviations of the mean correspond to 149, 330, and 374 ppm, respectively. Accuracies relative to triple-spike values are 149, 157, and 52 ppm, respectively, and thus well within uncertainties. The largest component of the uncertainties stems from the Pb data alone and is not caused by differential mass discrimination behaviour of Pb and Tl. In routine operation, variation of sample introduction memory and production of isobaric molecular interferences in the spectrometer's collision cell currently appear to be the ultimate limitation to better reproducibility.Comparative study of five different datasets from actual samples (bullets, international rock standards, carbonates, metamorphic minerals, and sulphide minerals) demonstrates that in most cases geological scatter of the sample exceeds the achieved analytical reproducibility. We observe good agreement between TIMS and MC-ICP-MS data for international rock standards but find that such comparison does not constitute the ultimate test for the validity of the MC-ICP-MS technique. Two attempted isochrons resulted in geological scatter (in one case small) in excess of analytical reproducibility. However, in one case (leached Great Dyke sulphides) we obtained a true isochron (MSWD = 0.63) age of 2578.3 ± 0.9 Ma, which is identical to and more precise than a recently published U–Pb zircon age (2579 ± 3 Ma) for a Great Dyke websterite [Earth Planet. Sci. Lett. 180 (2000) 1–12]. Reproducibility of this age by means of an isochron we regard as a robust test of accuracy over a wide dynamic range. We show that reliable and accurate Pb-isotope data can be obtained by careful operation of second-generation MC-ICP magnetic sector mass spectrometers.

Keywords: Pb-isotope; Analysis; Reproducibility; Isochron; Multi-collector inductively coupled plasma mass spectrometer

* Corresponding author. Fax: +61-7-3365-1277.
E-mail address: k.collerson@mailbox.uq.edu.au (K.D. Collerson).

0009-2541/02/$ - see front matter © 2002 Elsevier Science B.V. All rights reserved.
PII: S0009-2541(02)00059-1

1. Introduction

Over the last few years, a number of laboratories have demonstrated that multi-collector inductively coupled plasma mass spectrometers (MC-ICP-MS) are capable of precise and accurate Pb-isotope ratio measurements when samples are doped with Tl and mass discrimination is corrected relative to a certified $^{205}Tl/^{203}Tl$ ratio (Hirata, 1996; Belshaw et al., 1998; Rehkämper and Halliday, 1998; Rehkämper and Mezger, 2000). However, White et al. (2000) questioned whether Tl and Pb experienced similar fractionation behaviour. The principal aim of this study was to test mass bias behaviour of Tl and Pb in a second generation MC-ICP-MS and to demonstrate that the presently achieved accuracy is sufficient for most geological applications.

Claimed reproducibilities and accuracies for MC-ICP-MS Pb-isotope data constitute a significant improvement over conventional thermal-ionisation mass spectrometer (TIMS) data but they are presently not quite equivalent to high quality double and triple-spike data (e.g., Todt et al., 1996; Woodhead and Hergt, 1997; Galer and Abouchami, 1998; Thirlwall, 2000a). The aim of this paper is not to explore ways of closing the gap between these two techniques. We simply note that MC-ICP-MS technology provides an analytical time advantage that is important for laboratories that rely on significant commercial earnings for their existence. Furthermore, double- and triple-spike analyses require well-calibrated spikes and rely on ultra-clean filament loading procedures. These reasons may explain why those technologies are not widely applied.

Here we report an extensive set of Pb-isotope experiments with the University of Queensland (UQ) Micromass® Isoprobe© MC-ICP-MS conducted between June 1999 and February 2001. The paper has three specific goals:

(i) To document results of sample introduction experiments with a microconcentric nebuliser, which demonstrate that in routine operation, the memory of these devices contributes unfavourably to reproducibility. Some strategies to minimise memory effects are suggested.

(ii) To use raw (i.e., prior to mass discrimination correction) data for the NIST SRM 981 standard, obtained in 114 analytical sessions, to demonstrate that at least on the Micromass® Isoprobe©, combined Pb and Tl isotope measurements obey the same mass bias correction behaviour. There is no need to vary the normalisation factor on a daily basis (cf., Rehkämper and Mezger, 2000) or to apply empirical adjustments to the fractionation coefficient (White et al., 2000).

(iii) To demonstrate that we can reproduce the Pb-isotope compositions of natural samples by MC-ICP-MS over a wide dynamic range. Firstly, we compare Pb-isotope ratios of a simple matrix material (i.e., 32 calibre NORMA© bullets) with data obtained on the UQ TIMS. Secondly, we show comparative TIMS and MC-ICP-MS isotope ratios for rock standards BCR-2 and BHVO-2. We then report excellent reproducibility for a carbonate isochron using sample splits from a previously dated Archaean stromatolite and show geochronological data for metamorphic minerals using high precision common Pb multi-mineral regression techniques. Finally, we reproduce the well-established U–Pb zircon age of the Great Dyke (Zimbabwe) with a true, very precise Pb isochron obtained from progressively leached sulphides.

2. Experimental set-up

All measurements were performed on a Micromass® Isoprobe© equipped with 12 adjustable Faraday collectors under similar operating conditions to those reported by Rehkämper and Mezger (2000). The only differences concern the use of a Cetac® Aridus© desolvating nebuliser (compared to a Cetac® MCN 6000©) and the use of on-peak-zero correction prior to sample aspiration. This latter procedure involves a 60 s measurement of ion-currents of masses 202 through to 208 obtained from the same solvent (typically 2% HNO_3) in which the standard or sample is dissolved for later subtraction from the sample ion signal. On-peak-zero correction is essential for measurements performed with microconcentric nebulisers as it was found impossible to achieve a completely clean background (see next section for much more detail). The instrument is housed in a Class 10,000 clean laboratory at constant laboratory temperature (22 ± 0.5 °C) and ambient humidity ($50 \pm 10\%$). Full details of the laboratory design are given in Collerson (1995). The chiller temperature (for the magnet and ICP-interface) was initially set to 12 °C but as the

chiller is located in a non-air-conditioned room, it was difficult to maintain this temperature during the summer months. The temperature was therefore increased to 18 °C resulting in a significant improvement to magnet stability. Ions were collected in static mode on masses 202 through to 208. Hg-levels were found to be constant and reproducible for each tank of Ar gas (typically lasting 10–14 days). Tl from a commercial 1000 ppm ICP-MS standard solution was free of detectable Pb and Hg and was added to standards and samples immediately prior to analysis. Amplifier boards were calibrated with a reference signal on a weekly basis and were found to be stable within 6 ppm over the entire study period. Collector efficiencies were adjusted within 200 ppm of unity during initial set-up of the instrument to obtain consistent results for Nd, Hf, Os, Pb, and W standards. Best agreement for standards of all elements was found with collector efficiencies that vary systematically across the focal plane. Efficiencies have remained unchanged since original adjustment in 1999, indicating stability of Faraday cups and focal image. Seventy-two of the NIST SRM 981 datapoints were obtained during sessions dedicated only to standard measurements (initially NIST SRM 981 and 982, later 983). The remaining 42 datapoints were obtained as by-products of sample data acquisition. Typical total ion currents for Pb standards were $0.6–1.0 \times 10^{-10}$ A. The ratio of total Pb to Tl ion beam was varied between ca. 4 and 12 and no difference was found between the normalised Pb-isotope ratios.

Pb from silicate, carbonate, and sulphide samples was purified in HBr–HCl media by double-pass over miniaturised anion-exchange columns. Total blank levels remained below 20 pg and are negligible. Prior to final analysis, purified Pb from samples was dissolved in 1 ml 2% HCl, and Pb concentration levels were estimated from signal size of defocused ion beams. Samples were then typically further diluted (or redissolved in smaller amounts of acid) to achieve optimal total Pb ion currents of $0.4–0.6 \times 10^{-10}$ A and to ensure appropriate Tl spiking.

For Pb-isotope measurement of the bullets, two or three ca. 1-mm diameter holes were drilled in each projectile to localise the acid used to extract Pb. Each bullet was placed into a clean plastic beaker and washed in an ultrasonic bath using detergent, acetone, 2 N HCl and finally Milli-Q© water. Projectiles were then centrifuged and dried. Extraction of Pb from the bullets was achieved by addition of 5 μl of 7 N HNO_3 to each hole using a micropipette. After 2 h, the acid was evaporated to dryness on a hot plate at 75 °C. Pb nitrate was converted into Pb chloride using 7 μl of 6 N HCl and evaporated to dryness. For the TIMS analyses, the chloride residue was taken up with H_3PO_4 using a micropipette and loaded with Si-gel on a degassed Re filament for analysis. Isotope ratios were measured using static multi-collection using a VG 54-30 equipped with a pyrometer. Pb-isotope ratios were acquired at 1150–1350 °C. Isotope ratios were empirically corrected for instrumental mass fractionation of 0.9–1.5‰ per atomic mass unit depending on the ionisation temperature. These values were established by measuring replicate loads of NIST 981 at the beginning and at the end of a batch of seven samples. The amount of Pb required for each analysis was ca. 50–100 ng. The total Pb processing blank in the laboratory during the time that these analyses were obtained was ca. 10–20 pg and the blank introduced during sample loading onto the mass spectrometer filament was 20–50 fg. As these blanks are three to five orders of magnitude lower than the amount of Pb analysed, the blank contribution to the analyses of the bullets was negligible. Following TIMS analysis, there was sufficient Pb residue in the beakers for take-up in 2% HNO_3 for MC-ICP-MS analysis.

3. Sample introduction systems

Many basaltic rock samples and most mineral separates from crustal rocks have Pb concentrations ranging from 0.1 to 2 ppm. Separation of Pb from a 100-mg aliquot of such samples at best yields ca. 10–200 ng Pb. To obtain sufficient counting statistics for a high precision measurement by MC-ICP-MS, sub-100 ng samples need to be aspirated with a desolvating microconcentric nebuliser. These devices have the further advantage of producing relatively ‘dry’ plasma. They provide a relatively stable ion beam and can also be operated with a large variety of solvents. The present study used a newly purchased Cetac® Aridus© to replace a poorly performing MCN 6000©.

When coupled to a high sensitivity MC-ICP-MS, desolvating microconcentric nebulisers appear, however, to have unexpectedly persisting Pb 'memory', which contributes to an elevated working baseline that must be subtracted from the true sample ion current. Initial explanations for the source of this 'memory' Pb focused on parts of the system itself, in particular O-rings of the spray chamber assembly. However, our experience is that the persisting elevated baseline is a true memory effect from samples that were previously aspirated through the system. This can be demonstrated with the following two observations.

After replacement of O-rings and extensive cleaning, our Cetac® Aridus© was run for a period of 8 weeks specifically dedicated to the analysis of only two Pb-isotope standard solutions (NIST SRM 981 and 982). Memory effects became increasingly pronounced towards the end of this period of operation. The first indication of increased memory was that the time required for the sample signal to decay during wash out (ultrapure H_2O for 1 min, repeated once in separate H_2O, IPA (isopropyl alcohol) for 1 min, ultrapure 1% HF for 1 min, followed by 2% HNO_3) increased from ca. 8 to 40 min. Even after 40 min of washout, the baseline signal remained at 0.5–2.0×10^{-14} A on mass 208. This could be explained by contribution from reagent blank, sample introduction memory, ICP torch/lens memory, and isobaric interferences. Prior to analysis of a sample solution, we measured the baseline for later subtraction from the true sample ion current in a procedure known as on-peak-zero correction. By contrast, Rehkämper and Mezger (2000) applied the half mass unit baseline correction borrowed from TIMS protocol. This assumes that sample carryover or memory can be eliminated during washout, which in practice is impossible to achieve. On-peak-zero correction is thus important but only remains valid if the on-peak baseline measured at the beginning of an analysis remains constant during data collection and if no fluctuation of the electronic background occurs. In our laboratory with rigorous temperature and humidity control the latter factor is negligible.

Many users of MC-ICP-MS washout between samples until the signal has decayed to an empirically determined arbitrary threshold. This procedure is borrowed from quadrupole ICP-MS protocol. However, high-precision isotope ratio measurements are sensitive to very small memory effects particularly from samples with very different isotope compositions. We therefore prefer to washout until the isotope composition of the memory approaches a stable value. Our protocol is based on the following observations.

To test whether baselines decay to a stable background signal, major isotope ratios were measured during washout, as a stable background must, by definition, have constant isotope composition. Results of two such experiments are reported in Figs. 1 and 2. Fig. 1 shows the change in $^{208}Pb/^{206}Pb$ (panel A) and $^{207}Pb/^{206}Pb$ (panel B) after analysis of NIST SRM 981 as a function of washout time. There is a strong decrease in both isotope ratios. The isotope compositions became constant, within analytical error, only after a washout period of 40 min. $^{208}Pb/^{206}Pb$ (Fig. 2A) and $^{207}Pb/^{206}Pb$ (Fig. 2B) isotope ratios measured

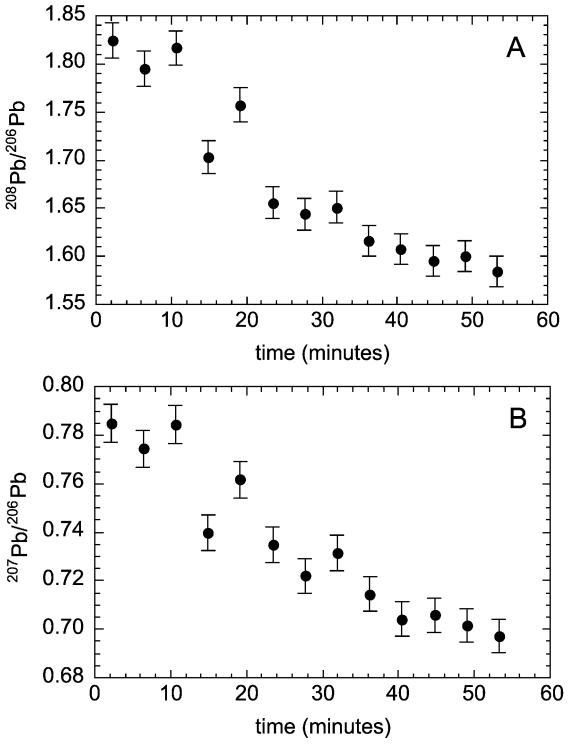

Fig. 1. Temporal evolution of $^{208}Pb/^{206}Pb$ (panel A) and $^{207}Pb/^{206}Pb$ (panel B) ratios measured during washout after analysis of NIST SRM 981. Data were obtained with the same on-peak-zero correction and peak centering as the preceding standard measurement. Each datapoint corresponds to a block of eight measurements, each integrating over 30 s.

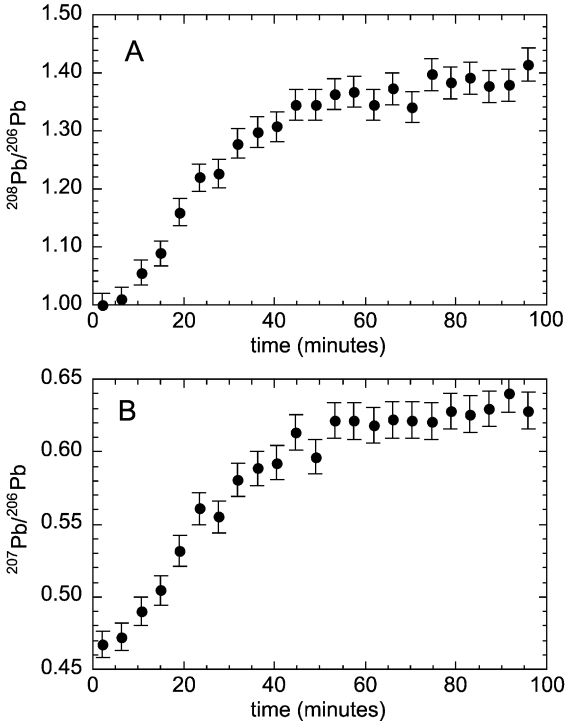

Fig. 2. Temporal evolution of $^{208}Pb/^{206}Pb$ (panel A) and $^{207}Pb/^{206}Pb$ (panel B) ratios measured during washout after analysis of NIST SRM 982. Data were obtained with the same on-peak-zero correction and peak centering as the preceding standard measurement. Each datapoint corresponds to a block of eight measurements, each integrating over 30 s.

during wash-out after analysis of NIST SRM 982, however, showed a marked increase with time and also levelled out after ca. 40 min. This was subsequently verified by a longer (100 min) washout experiment. The observation of opposite change of isotope ratio for NIST SRM 981 and 982 suggests that the isotope composition of the memory is intermediate between the two standards. When plotted in a $^{208}Pb/^{206}Pb$ and $^{207}Pb/^{206}Pb$ diagram (Fig. 3A), it is obvious that the datapoints from both washouts define a linear trend that indicates binary mixing. Most importantly, the mixing line (which was defined by the wash-out measurements only) extrapolates to NIST SRM 982 at the lower end, and NIST SRM 981 at the higher end. The most likely explanation of this observation is that the Pb that contributes to the working baseline is a mixture of Pb previously run on the system. As no Pb from natural samples had been analysed at that time, the baseline Pb data reflects simple binary mixing. The only alternative explanation for this observation would be that the Cetac® Aridus© or our reagents contained a blank with a Pb-isotope composition that fortuitously plotted somewhere around the centre of the mixing line. However, because of the very unusual isotope composition of NIST SRM 982 (i.e., equal 206 and 208 atom Pb), the isotope composition of the proposed contaminant would also have to be very unusual and very different from 'common' Pb, which resembles the composition of NIST SRM 981. Nevertheless, the isotope composition of the Pb blank of commercial nitric acid was determined. The concentrated nitric acid was diluted

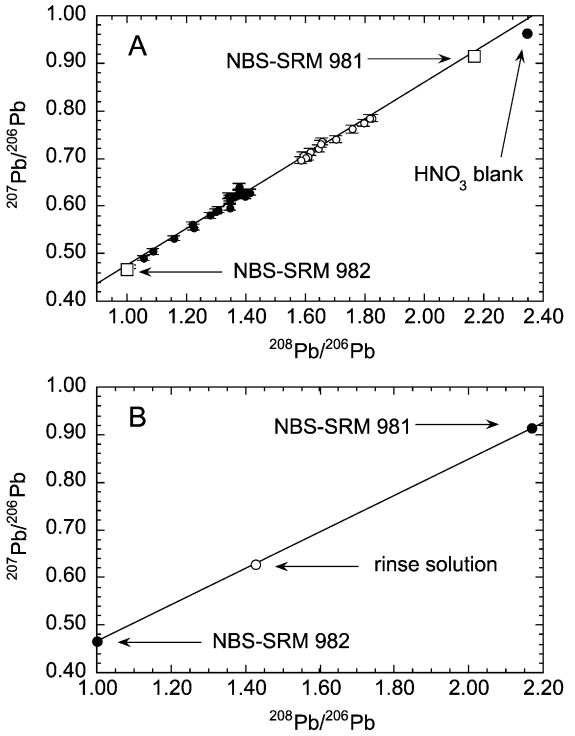

Fig. 3. (A) Plot of $^{208}Pb/^{206}Pb$ versus $^{207}Pb/^{206}Pb$ ratios measured during washout after analysis of NIST SRM 981 (open circles) and NIST SRM 982 (solid circles). A linear regression ($r^2 = 0.993$) extends exactly to the standard compositions (open large squares). The Pb-isotope composition determined for commercial nitric acid is plotted for comparison. (B) Identical plot showing isotope composition (large open circle) of cleaning acid (ultra-pure 2% HNO_3) recovered from Cetac® Aridus© after soaking. An excellent linear fit ($r^2 = 0.9999$) connects the recovered acid's isotope composition with those of NIST SRM 981 and 982.

to 2% with the same high purity water (with undetectable Pb-blank) that was used to dilute the NIST standards. Even this diluted commercial undistilled nitric acid only yielded a blank of 5 ppt, which did not contribute significantly to the baseline. The Pb-isotope composition of Pb from the nitric acid had to be determined on a dried-down aliquot of 100 ml concentrated acid. The blank's Pb-isotope composition (shown on Fig. 3A) is, not surprisingly, very similar to Mid-Proterozoic Pb from the main Pb producing mines in Australia (Broken Hill and Mt. Isa) and could therefore not explain the isotope composition of the baseline.

After 8 weeks of operation, the Cetac® Aridus© was cleaned using the rinse kit that was provided. The washout reagent was recovered and the isotope composition of the Pb memory was determined from the rinse solution. Prior to rinsing, the Cetac® Aridus© was flushed with ultra-clean 2% HNO_3 for 2 h. The system was then switched off, the spray chamber was removed and leached in warm 3% HNO_3 for 2 h. After replacing the spray chamber and cleaning the rinse kit, 400 ml of ultra-clean 2% HNO_3 were flushed into the Cetac® Aridus© and left soaking for 1 h. A total of 370 ml of the rinse solution was recovered. Its Pb concentration was determined to 2.87 ppb by quadrupole ICP-MS. Hence, the total amount of Pb recovered in the (400 ml) rinse solution was ca. 1150 ng. This compares unfavourably with typical sample amounts of 20–40 ng. In other words, the Cetac® Aridus© system (prior to rinsing) contained 30–60 times more Pb than a typical sample. The isotope composition of Pb in the recovered acid was easily measured by MC-ICP-MS due to the fact that the rinse solution also contained Tl, allowing for mass bias correction. As shown on Fig. 3B, the Pb in the rinse solution had a very peculiar isotope composition that plots exactly on a mixing line defined by NIST-SRM 981 and 982. Thus it is clear that the Pb recovered in the rinse solution was leached from the Cetac® Aridus© itself (possibly the teflon membranes), and not from the rinsing kit. From our logbook records, we calculated that no more than 18,000 ng of Pb had been aspirated during the 8 weeks operation (no other standards of other elements were run during this time). The fact that ca. 1150 ng of Pb was recovered in a single rinse means that at least 6% of the Pb that was aspirated through the Cetac® Aridus© was retained.

To minimise such memory effects, we have adopted washout protocols that use stronger acids (10% nitric acid and 2% hydrofluoric acid) for periods between 10 and 20 min. In addition, repeated rinses of the entire system are performed each week. Nevertheless, routine measurements of element concentration in recovered rinse solutions consistently show that significant levels (i.e., >1000 ng) of Pb and other analysed elements (such Re and Os) appear to become deposited in some parts of the desolvating nebuliser. Our largest current working baseline (i.e., the on-peak-zero correction) is found on mass 208 and typically ranges between 2 and 3.5×10^{-15} A. Relative to a typical run signal of 3×10^{-11} A on mass 208, the on-peak-zero correction thus amounts to between 65 and 115 ppm. Because the washout behaviour of real samples differs markedly from that of pure solutions (probably due to matrix effects), utmost care must therefore be taken to ensure that a stable background is achieved after washout. Since wash-out behaviour is clearly a function of sample matrix (i.e., Ca-bearing samples, such as carbonates and plagioclase, appear to have much better washout and uptake characteristics than FeMg-rich samples) there is a real possibility that samples could carry over more memory Pb than the 2% HNO_3 that is used to determine the on-peak-zero signal. There is the added complication that higher sample viscosity (affecting the real vs. nominal sample up-take and gas flow rate through the microconcentric nebuliser) and more complex matrix could lead to production of isobaric molecular interferences in the hexapole collision cell. In-run fluctuation of the combined background (memory and isobaric interferences) is an obvious limitation to even better reproducibility of standard analysis. Measures to optimise background fluctuations include:

(i) minimisation of solute amounts aspirated through the nebuliser;
(ii) baseline stability control by monitoring signal size on ion-counter or by measuring baseline isotope ratios (Figs. 1 and 2);
(iii) on-peak-zero measurement for at least 60 s;
(iv) exactly matching the acid strength between sample solution and on-peak-zero blank acid;

(v) use of high purity samples (as for TIMS) to avoid adverse effects of matrix elements, particularly Fe and Mg, on washout time;
(vi) overnight clean-out of system by aspiration of relatively strong acids such as 10% HNO_3 or 1% HF; and
(vii) overnight bake-out of hexapole collision cell to minimise formation of molecular species.

4. Data for NIST SRM 981

4.1. Introduction

Previous studies of Pb-isotope analysis by MC-ICP-MS have achieved reproducibilities of ca. 50–200 ppm for the $^{207}Pb/^{206}Pb$ and $^{208}Pb/^{206}Pb$ ratios and 100–400 ppm for the ^{204}Pb-based ratios (see, e.g., compilation by Rehkämper and Mezger, 2000). Such reproducibility is a very significant improvement over that achieved by conventional TIMS measurements and is more than adequate for addressing a very wide array of geological problems that were inaccessible with conventional data. Nevertheless, the reproducibility achieved by Tl-doped MC-ICP-MS technique appears inferior to that achieved by double- or triple-spike TIMS technique (e.g., Todt et al., 1996; Galer and Abouchami, 1998; Thirlwall, 2000a). One explanation suggested for this inferior reproducibility is that in reality, mass discrimination might not be completely element-independent and that 'external' correction of Pb mass discrimination with Tl is the ultimate limitation to better reproducibility (e.g., White et al., 2000). That line of reasoning, although rarely explicitly stated, would explain why different laboratories report quite different $^{205}Tl/^{203}Tl$ ratios for normalisation. Indeed, the proposed $^{205}Tl/^{203}Tl$ ratios range from 2.3865 (lowest value of Rehkämper and Mezger, 2000), 2.3871 (Hirata, 1996; White et al., 2000), 2.3875 (Belshaw et al., 1998), 2.38869 (this study), to 2.38881 (Rehkämper and Halliday, 1998). This range corresponds to 967 ppm, which still is within IUPAC uncertainties. The implicitly assumed source of uncertainty is an inferred slight deviation in mass discrimination behaviour between Tl and Pb. We next test that hypothesis with our own extensive dataset for NIST SRM 981 obtained at UQ (summary data in Table 1).

4.2. Mass discrimination behaviour

Mass discrimination that occurs between sample introduction and ion collection in an MC-ICP-MS has been successfully described by both the power and the exponential laws. Several studies found very little difference between values corrected with either law. Before testing whether mass discrimination of Pb can be approximated by that of Tl, it is necessary to test whether raw (i.e., only corrected of Hg-interference) Pb data alone obey the power- and/or exponential laws. A convenient test of that hypothesis is to plot the raw data in log–log or ln–ln space. If mass discrimination is governed by those laws, the datapoints must define straight lines in these plots. Importantly, the slopes of correlation lines are purely a function of the relative mass differences, and not of the isotope ratio of the standard or sample in question (Maréchal et al., 1999). This means that power- or exponential-law behaviour can be tested without knowledge of the isotope composition. For exponential law, the $^{208}Pb/^{206}Pb$ vs. $^{207}Pb/^{206}Pb$ slope is defined as

$$\text{slope} = \frac{\log(M_{208}/M_{206})}{\log(M_{207}/M_{206}),} \quad (1)$$

where M refers to the atomic mass. The intercept, on the other hand, depends on the relative mass difference as well as on the absolute values of the isotope ratios. For exponential law, the $^{208}Pb/^{206}Pb$ vs. $^{207}Pb/^{206}Pb$ intercept is defined as

$$\text{intercept} = \left[\log\left(\frac{^{208}Pb}{^{206}Pb}\right)_{true} - \frac{\log\left(\frac{M_{208}}{M_{206}}\right)}{\log\left(\frac{M_{207}}{M_{206}}\right)} \times \log\left(\frac{^{207}Pb}{^{206}Pb}\right)_{true}\right]. \quad (2)$$

Fig. 4A shows a $\log(^{208}Pb/^{206}Pb)$ vs. $\log(^{207}Pb/^{206}Pb)$ plot for NIST SRM 981 standard data. The first observation is that the data can be successfully fitted with a linear regression (r^2 of 0.995). The slope of the regression line is 2.004 ± 14, which, within error, is identical to the theoretical slope of 1.9945. Rehkämper and Mezger (2000) found that the stability of mass discrimination typically seen on the Micromass® Isoprobe© over a daily analytical session precluded calculation of meaningful regression parameters. Our extensive dataset (114 datapoints obtained over 14

Table 1
Pb isotope data

Standard or sample name	$^{207}Pb/^{206}Pb$	±	$^{208}Pb/^{206}Pb$	±	$^{206}Pb/^{204}Pb$	±
NIST SRM 981						
This study (average of 114 analyses)	0.91461	18	2.16740	70	16.941	6
This study (internal Pb normalisation)	0.91466	12	2.16771		16.943	5
Galer and Abouchami (1998)	0.91475	4	2.16771	10	16.941	2
Thirlwall (2000a,b)	0.91469	7	2.16770	21	16.941	2
NIST SRM 982						
This study (average of 14 analyses)	0.46703	8	1.00026	11	36.754	9
Norma® bullets						
Batch #1 MC-ICP-MS	0.86517	2	2.11362	12	18.147	3
Batch #1 TIMS	0.86610	27	2.11570	79	18.197	4
Batch #2 MC-ICP-MS	0.81936	1	2.00770	8	19.214	1
Batch #2 TIMS	0.82023	14	2.00554	34	19.254	6
Batch #3 MC-ICP-MS	0.89338	1	2.14143	6	17.377	1
Batch #3 TIMS	0.89430	6	2.14250	43	17.386	2
Batch #4 MC-ICP-MS	0.77025	2	1.90968	9	20.671	2
Batch #4 TIMS	0.77071	16	1.90876	74	20.684	6
Batch #5 MC-ICP-MS	0.76385	1	1.89438	8	20.871	1
Batch #5 TIMS	0.76340	14	1.89330	80	20.890	8
USGS standard data						
BCR-2 #1	0.83272	1	2.06385	4	18.764	1
BCR-2 #2	0.83276	2	2.06412	7	18.755	1
BCR-2 #3	0.83278	2	2.06429	6	18.752	1
BHVO-2 #1	0.83290	2	2.04921	7	18.680	1
BHVO-2 #2	0.83288	2	2.04917	7	18.679	1
Mushandike limestone samples						
Core section #5	0.47082	4	1.06177	20	49.862	9
Core section #7	0.48338	2	1.09023	16	47.125	7
Core section #9	0.64170	1	1.40922	12	30.169	2
Core section #11	0.57980	2	1.27518	14	35.301	4
Core section #13	0.50950	2	1.14452	15	42.928	6
Core section #15	0.50923	2	1.13688	16	42.860	6
Core section #17	0.48738	2	1.10160	15	45.797	6
Core section #19	0.51324	1	1.18274	10	42.263	4
Core section #21	0.32678	1	0.71290	7	104.365	11
Core section #23	0.46725	1	1.05915	10	49.338	4
NIST SRM 983						
This study (average of four measurements)	0.07152	6	0.01391	7	2700.4	19.5
S. Bowring (personal communication, 2000)	0.07116		0.01366		2695.4	
Amphibolite mineral isochron						
Plagioclase	1.12745	5	2.64469	20	12.047	1
Whole rock	1.10024	5	2.58669	18	12.484	1
Apatite	0.97402	5	2.35493	16	14.656	1
Sphene #1	0.27597	1	1.02330	41	310.11	12
Sphene #2	0.26040	4	1.05958	417	575.07	2.26

Table 1 (*continued*)

Standard or sample name	$^{207}Pb/^{206}Pb$	±	$^{208}Pb/^{206}Pb$	±	$^{206}Pb/^{204}Pb$	±
Sulphide concentrate isochron						
Leachte #1 (1 M HBr)	1.01198	4	2.34326	16	15.045	1
Leachte #2 (3 M HBr)	1.00174	8	2.29234	21	15.233	2
Leachte #3 (aqua regia, 3 h)	0.68890	3	1.50385	12	24.459	2
Leachte #4 (aqua regia, 12 h)	0.30404	2	0.54036	16	95.792	20

Tabulated uncertainties for samples are absolute two sigma internal errors (standard errors). Quoted uncertainties for NIST standards are absolute two sigma reproducibilities (standard deviations).

months), however, shows a larger spread in absolute mass discrimination, which was partly achieved by repositioning of the torch, small variation to the hexapole collision gas flow, and modified sample up-take rate. Although the increased spread in our data allows a better definition of slope and intercept we prefer, in practice, to fit the data to the theoretical slope, because we explicitly assume ideal exponential law fractionation behaviour. In that case, the true slope of our data array *must* correspond to the theoretical slope of 1.9945. Fig. 4B shows that there is insignificant difference between the free-fit and the forced-fit (to the theoretical slope). Furthermore, the slope defined by our data projects closely to normalised literature data, which means that given adequate normalisation, it should be possible to obtain accurate isotope data. Identical observations were made for $^{206}Pb/^{204}Pb$ vs. $^{207}Pb/^{206}Pb$ data (Fig. 5), although the correlation coefficient of that regression line (r^2 of 0.986) is slightly inferior due probably to the fact that mass 204 yields a much smaller ion current and also requires a small Hg-interference correction. Nevertheless, both datasets demonstrate that mass discrimination of Pb-isotopes can be successfully described by the exponential law. Virtually identical results could be obtained with the power law but will not be further discussed in this paper.

4.3. Internally normalised data

Before testing whether mixed Tl–Pb isotope data also obey the power law, it is essential to determine the reproducibility that could be achieved if Pb had a stable isotope ratio. For that purpose, we calculated the mass discrimination factor by comparing the measured with the known $^{208}Pb/^{206}Pb$ ratio (in this case 2.16771; Galer and Abouchami, 1998, which is identical to the value subsequently reported by Thirlwall, 2000a) of all our NIST SRM 981 data. The resulting mean $^{207}Pb/^{206}Pb$ and $^{206}Pb/^{204}Pb$ ratios are 0.914666 ± 115 and 16.9430 ± 51, respectively (Table 1). The quoted reproducibilities are two sigma standard deviations and correspond to 126 and 303 ppm, respectively. Both mean values are, within error, accurate relative to the Galer and Abouchami (1998) and Thirlwall (2000a) data. While the $^{208}Pb/^{206}Pb$ normalised $^{207}Pb/^{206}Pb$ and $^{206}Pb/^{204}Pb$ data demonstrate that mass discrimination is well-corrected by exponential law the two sigma standard deviations show that irrespective of Tl-based mass discrimination, reproducibility of MC-ICP-MS Pb-isotope measurements is limited by Pb ion current collection. The 126 ppm reproducibility for the internally corrected $^{207}Pb/^{206}Pb$ ratio is inferior to the <20 ppm two sigma reproducabilities obtained on the UQ instrument for other internally corrected ratios (e.g., $^{182}W/^{183}W$; Schoenberg et al., in press). In our experience, a number of factors contribute. Firstly, in order to maximise sample throughput, we limit Pb acquisition time to 8 min for samples with total Pb ion beams $>2 \times 10^{-11}$ A, because the reproducibility and accuracy that we achieve with this strategy is generally better than the degree of geological scatter of typical samples (as shown below). Acquisition times of 30–40 min improve reproducibility by a factor of ca. 2, but in routine operation the advantage of better reproducibility is offset by the much-increased wash-out time required to minimise memory. Secondly, because Pb shows a much stronger memory effect on our microconcentric nebuliser than other elements like W or Hf, on-peak-zero correction amounts to 50–100 ppm of total signal, compared to 5–20 ppm for W and Hf. The gradual deposition of substantial amounts of aspirated Pb was not observed for other investigated elements. Thirdly, without bake-out of the hexapole collision cell, the baseline in the Pb mass

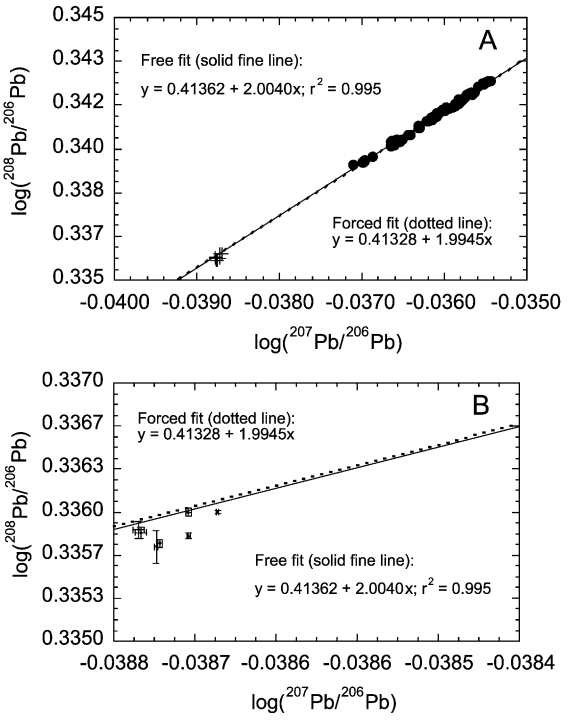

Fig. 4. Raw isotope data ($n=114$) for NIST SRM 981 on log–log scale. (A) $^{208}Pb/^{206}Pb$ versus $^{207}Pb/^{206}Pb$ plot shows individual datapoints (full circles) fitted with a linear regression (free fit, solid fine line) and with a regression (dotted fat line) to the forced theoretical slope of 1.9945. Note the insignificant difference between the two regression lines and the correct projection to literature values for NIST SRM 981 (cross symbols). (B) Detail of (A) showing the difference between the free (solid fine line) and the forced (fat dotted line) fits in the range of the true, unfractionated values of NIST SRM 981. Both fits extend along the upper limit of literature values (Todt et al., 1996; Hirata, 1996; Galer and Abouchami, 1998; Rehkämper and Halliday, 1998, Belshaw et al., 1998; Rehkämper and Mezger, 2000; Thirlwall, 2000a,b). Best agreement is found with the double and triple-spike data of Thirlwall (2000a,b) and Galer and Abouchami (1998), respectively.

range on our MC-ICP-MS becomes noisier than at lower mass and develops small (i.e., $<1\times10^{-15}$ A) but discernible peaks which due to their relative abundance, cannot be caused by Pb blank or memory. Thirlwall (2000b) proposed that abundance sensitivity was the major problem affecting MC-ICP-MS Pb-isotope analysis. However, over the period of operation, the abundance sensitivity on our instrument as measured from the ^{238}U tail on mass 237 remained low (≤ 10 ppm) and, more importantly stable as indicated by a stable analyser pressure ($\leq 2.87\times10^{-8}$ mbar) over more than 3 years of operation of the MC-ICP-MS. Abundance sensitivity could only explain the observed scatter, if it changed over daily to weekly periods (Thirlwall, 2000b) or if standards with different $^{206}Pb/^{205}Tl$ were measured. Finally, abundance sensitivity problems would also be expected to affect isotope measurements of other elements to a similar extent. This was neither observed in our laboratory (Schoenberg et al., in press) nor at the University of Münster (Münker et al., 2000; Scherer et al., 2001) who operate an identical instrument. However, there is a possibility that our instrument has better abundance sensitivity than the results of Rehkämper and Mezger

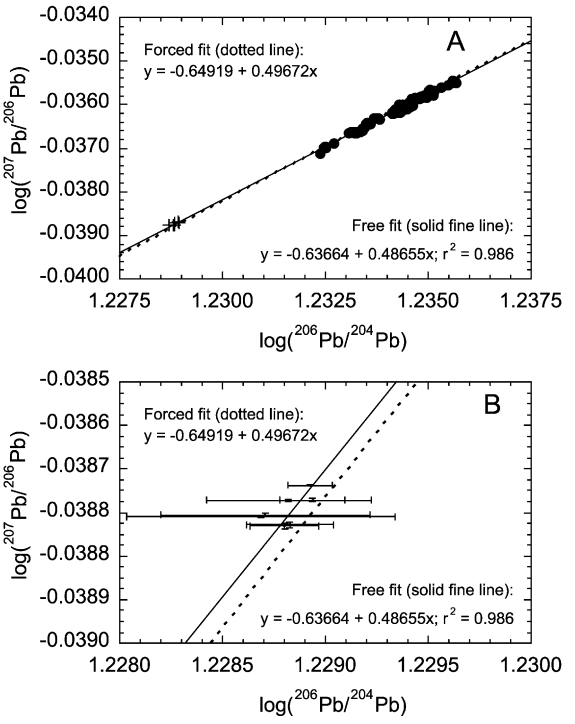

Fig. 5. Raw (^{204}Hg-corrected) isotope data ($n=114$) for NIST SRM 981 on log–log scale. (A) $^{206}Pb/^{204}Pb$ versus $^{207}Pb/^{204}Pb$ plot shows individual datapoints (full circles) fitted with a linear regression (free fit, solid fine line) and with a regression (dotted fat line) to the forced theoretical slope of 0.49672. Note the insignificant difference between the two regression lines and the correct projection to literature values for NIST SRM 981 (cross symbols). (B) Detail of (A) showing the difference between the free (solid fine line) and the forced (fat dotted line) fits in the range of the true, unfractionated values of NIST SRM 981. Both fits extend right into the cluster of literature values (same sources as for Fig. 4).

(2000) suggest. Possibly more effective bake-out of hexapole collision cell (to reduce production of isobaric molecular species) may contribute to this behaviour.

4.4. Thallium normalised data

The first step for external Tl-based normalisation is to plot the raw (only Hg-interference corrected) Pb-isotope ratios against that of Tl. Fig. 6 demonstrates that in log–log plots for the three independent Pb-isotope ratios, the data define very good linear correlations (r^2 from 0.988 to 0.992). The slopes of the Pb–Tl regression lines are, within error, identical with the theoretical predictions and cannot be distinguished from fits to the data with forced slopes (Fig. 6). Provided the true Pb-isotope ratios of NIST SRM 981 are known, the equations of the forced regression lines can be solved for the $^{205}Tl/^{203}Tl$ ratio. Relative to the Galer and Abouchami (1998) values for NIST SRM 981 we obtain the following three $^{205}Tl/^{203}Tl$ ratios: 2.38909 (from the $^{207}Pb/^{206}Pb$ data); 2.38856 (from the $^{208}Pb/^{206}Pb$ data); and 2.38843 (from the $^{206}Pb/^{204}Pb$ data). The mean value of 2.38869 ± 70 is identical to 2.38881 obtained by Rehkämper and Halliday (1998). Normalising all our NIST SRM 981 data with $^{205}Tl/^{203}Tl$ of 2.38869 yielded the following averages and reproducibilities (Fig. 7): $^{207}Pb/^{206}Pb = 0.91461 \pm 18$; $^{208}Pb/^{206}Pb = 2.1674 \pm 7$; 7; and $^{206}Pb/^{204}Pb = 16.941 \pm 6$ (Table 1). The quoted two sigma standard deviations of the mean correspond to 149, 330, and 374 ppm, respectively. Accuracies relative to the Galer and Abouchami (1998) values are 149, 157, and 52 ppm, respectively, and thus well within the uncertainties. Accuracies relative the Thirlwall (2000a) values are 87, 143, and 6 ppm, respectively. We therefore conclude that there is no significant element-specific component to mass discrimination, allowing for accurate correction of Pb-

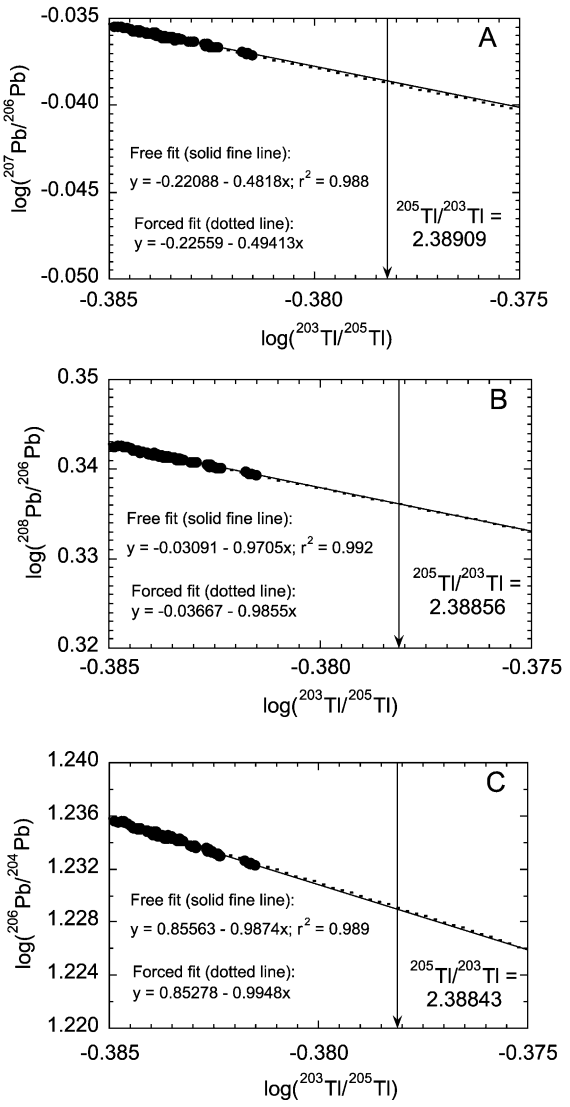

Fig. 6. Raw (^{204}Hg-corrected) Tl-doped Pb-isotope data ($n = 114$) for NIST SRM 981 on log–log scale. (A) $^{207}Pb/^{206}Pb$ versus $^{203}Tl/^{205}Tl$ isotope ratio plot shows individual datapoints (full circles) fitted with a linear regression (free fit, solid fine line) and with a regression (dotted fat line) to the forced theoretical slope of −0.49413. Note the insignificant difference between the two regression lines. Relative to a true $^{207}Pb/^{206}Pb$ ratio of 0.91475 (Galer and Abouchami, 1998) a $^{205}Tl/^{203}Tl$ ratio of 2.38909 is calculated from the forced fit. (B) $^{208}Pb/^{206}Pb$ versus $^{203}Tl/^{205}Tl$ isotope ratio plot shows individual datapoints (full circles) fitted with a linear regression (free fit, solid fine line) and with a regression (dotted fat line) to the forced theoretical slope of −0.9855. Note the insignificant difference between the two regression lines. Relative to a true $^{208}Pb/^{206}Pb$ ratio of 2.16771 (Galer and Abouchami, 1998) a $^{205}Tl/^{203}Tl$ ratio of 2.38856 is calculated from the forced fit. (C) $^{206}Pb/^{204}Pb$ versus $^{203}Tl/^{205}Tl$ isotope ratio plot shows individual datapoints (full circles) fitted with a linear regression (free fit, solid fine line) and with a regression (dotted fat line) to the forced theoretical slope of −0.9948. Note the insignificant difference between the two regression lines. Relative to a true $^{206}Pb/^{204}Pb$ ratio of 16.9405 (Galer and Abouchami, 1998) a $^{205}Tl/^{203}Tl$ ratio of 2.38909 is calculated from the forced fit.

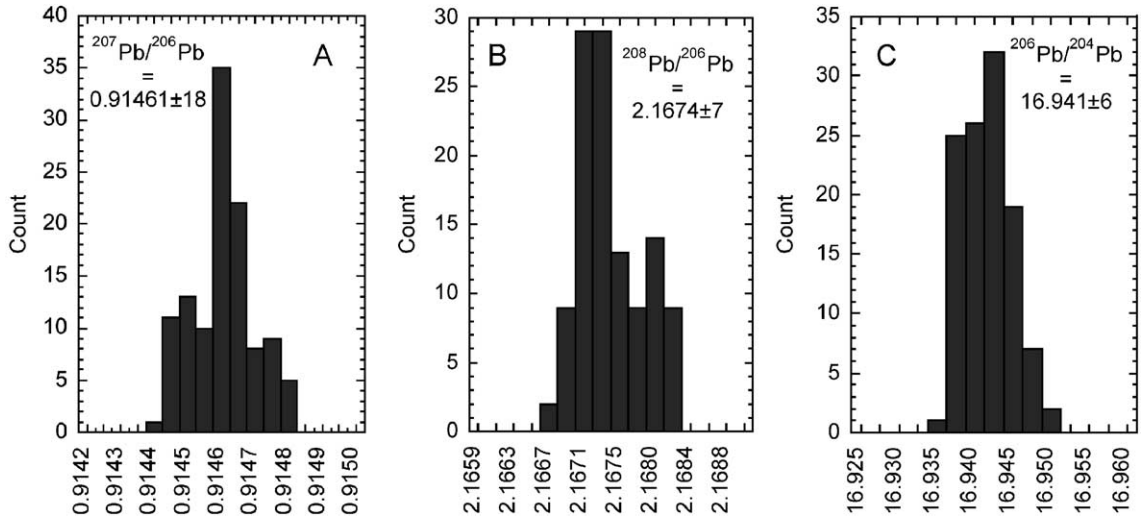

Fig. 7. Histograms of Pb-isotope ratios for NIST SRM 981 normalised to $^{205}Tl/^{203}Tl$ ratio of 2.38869. (A) $^{207}Pb/^{206}Pb$ values showing mean and the absolute two-sigma standard deviation. (B) $^{208}Pb/^{206}Pb$ values showing mean and the absolute two-sigma standard deviation. (C) $^{206}Pb/^{204}Pb$ values showing mean and the absolute two-sigma standard deviation.

isotope data with Tl. The largest component of the uncertainties stems from the Pb data alone and is not caused by differential behaviour of Pb and Tl.

The quoted reproducibilities are higher than those reported by some of the earlier studies. Rehkämper and Halliday (1998) quoted two sigma reproducibilities of 48, 52, and 270 ppm for $^{207}Pb/^{206}Pb$, $^{208}Pb/^{206}Pb$, and $^{206}Pb/^{204}Pb$ ratios, respectively (Table 1). However, as those authors state (p. 131) they "applied a 2 sigma filter to their dataset in order to identify outliers". Our dataset, on the other hand, reports the full reproducibilities of a much larger unfiltered dataset ($n = 114$ cf. $n = 30$) as we do not believe that rejection of outliers is permissible to determine reliable reproducibility for elements with no constant isotope ratio. Regardless, in terms of accuracy (in their case relative to the NIST SRM 981 values reported by Todt et al., 1996) our results are comparable to those of Rehkämper and Halliday (1998) whose estimates of accuracies are much larger than their reproducibilities. In a more recent study, Rehkämper and Mezger (2000) claim reproducibilities of 142, 133, and 172 ppm for $^{207}Pb/^{206}Pb$, $^{208}Pb/^{206}Pb$, and $^{206}Pb/^{204}Pb$ ratios, respectively (Table 1). Our own reproducibilities are again a factor of ca. 2 larger. However, Rehkämper and Mezger (2000) did not use a constant $^{205}Tl/^{203}Tl$ ratio but determined an 'optimised' value for each measurement session. We disagree with such practice for two reasons. Firstly, the range in $^{205}Tl/^{203}Tl$ values used by Rehkämper and Mezger (2000) spans 377 ppm, which is substantially larger than their quoted reproducibility of the $^{206}Pb/^{204}Pb$ ratio (172 ppm). We question the confidence with which an 'optimised' value for $^{205}Tl/^{203}Tl$ is seen as valid over the entire measurement session. Secondly, and more importantly, there is simply no physical rationale for changing the $^{205}Tl/^{203}Tl$ ratio so long as Tl from a common stock is being added to samples. This is best illustrated with reference to our Fig. 6, where the raw Pb-isotope ratios are plotted against the Tl ratio. Eq. (1) states that the slope in such a diagram is defined by the relative mass differences. Eq. (2) states that the intercept depends on both the relative mass differences and the absolute isotope compositions of the two elements. In the case of a mixture of two standard solutions, both slope and intercept are fixed. By 'optimising' the $^{205}Tl/^{203}Tl$ ratio, Rehkämper and Mezger (2000) in effect shift the intercept defined by Eq. (2) in order to remove some of the scatter about a single regression line. While this approach may yield better reproducibilities it clearly violates physical principles. Rehkämper and Mezger (2000) justify their procedure by claiming that the range in 'optimised' $^{205}Tl/^{203}Tl$ ratios did not exceed the uncertainty with which the isotope compo-

sition of terrestrial Tl is known. However, the crucial point is that the $^{205}Tl/^{203}Tl$ ratio of their standard solution is *constant*, no matter how well it is known. In other words, for a mixture of two standards, both Eqs. (1) and (2) are known and cannot be varied. In view of the fact that we use a single $^{205}Tl/^{203}Tl$ ratio for our entire dataset, our quoted, unfiltered reproducibilities are not only more realistic but also better than those obtained by Rehkämper and Mezger (2000).

Finally, White et al. (2000) reported problems with Tl-normalised Pb-isotope measurements. Those authors claimed that on their first generation MC-ICP-MS, mass discrimination behaviour of Tl and Pb is not identical. However, we first notice (on their Fig. 1) that there is a very large difference between data of their two measurement sessions. Such large variations are not seen in our dataset (obtained over a much longer time span), which may reflect problems with the raw data reported in White et al. (2000). We are not convinced that such scattered data can be used to claim differential mass discrimination behaviour of Pb and Tl. Furthermore, the range of mass discrimination of their data is only half of that observed by us, which makes our regression results more robust. Lastly, White et al. (2000) did not demonstrate that their Pb data alone showed the expected power law (or in their case, exponential law) mass discrimination.

In brief, our experiments with NIST SRM 981 show that Tl-normalised MC-ICP-MS Pb-isotope analysis is feasible and yields results of better accuracy and precision than conventional TIMS data. Our procedure can successfully be used to obtain accurate results without the need for changing the Tl normalisation ratio or for postulating differential fractionation coefficients for Tl and Pb. Similar reproducibility and accuracy were achieved for NIST SRM 982 (Table 1). Accuracy and reproducibility achieved in this study fall short of predictions from measurement of other elements (e.g., W; Schoenberg et al., in press). Accuracy of NIST SRM 982 data relative to Todt et al. (1996) is 3 ppm for $^{207}Pb/^{206}Pb$, 95 ppm for $^{208}Pb/^{206}Pb$, and 114 ppm for $^{206}Pb/^{204}Pb$. In the remaining section of this paper we report data from samples from a variety of matrices over a large dynamic range to test whether MC-ICP-MS technique is equally suitable for Pb-isotope analysis of natural samples.

5. Reproducibility of non-standard materials

5.1. Bullet Pb data

A first experiment to test our ability to reproduce TIMS data with the MC-ICP-MS technique focussed on a simple sample matrix. For this purpose, projectiles from five different batches of Norma® 32 calibre ammunition were dissolved and both TIMS and MC-ICP-MS analyses were performed without chemical purification of Pb. Pb-isotope ratios of bullets vary according to the composition of the scrap Pb used to produce a particular batch of bullets. Unfortunately, it is impossible to estimate the amount of Pb loaded onto the TIMS filament such that analyses had to be performed over a much wider range of nominal filament temperatures than that used for standards. Data are given in Table 1 and presented on Fig. 8, which demonstrates that the $^{207}Pb/^{206}Pb$ and $^{208}Pb/^{206}Pb$ ratios were reproduced within ca. 1.2 per mil uncertainty. However, $^{206}Pb/^{204}Pb$ ratios for two of the five samples differed outside the 1.2 per mil, which is the typical reproducibility of this ratio obtained from repeat analyses of NIST SRM 981. We attribute this to inaccuracy of the TIMS data caused by the wide range of nominal filament temperatures over which the samples had to be measured. As such, the bullet data exemplify the limited use of comparing conventional TIMS with MC-ICP-MS or triple-spike data, because reproducibility of non-standard data may be significantly larger than that estimated by repeat analyses of standards of known concentration (see also Woodhead and Hergt, 1997).

5.2. Rock standards

Very few precise and accurate measurements for international rock standards have so far been published and little is known about the isotope homogeneity of such standards. Woodhead and Hergt (2000) recently reported the first Pb-isotope data for USGS samples obtained with a double-spike procedure. Their study found isotopic differences between first and second-generation standards, which are also reflected in Pb concentration values. We performed a study of BCR-2 (three separate aliquots) and BHVO-2 (two aliquots). Each aliquot was treated as a separate sample, which were digested in high-

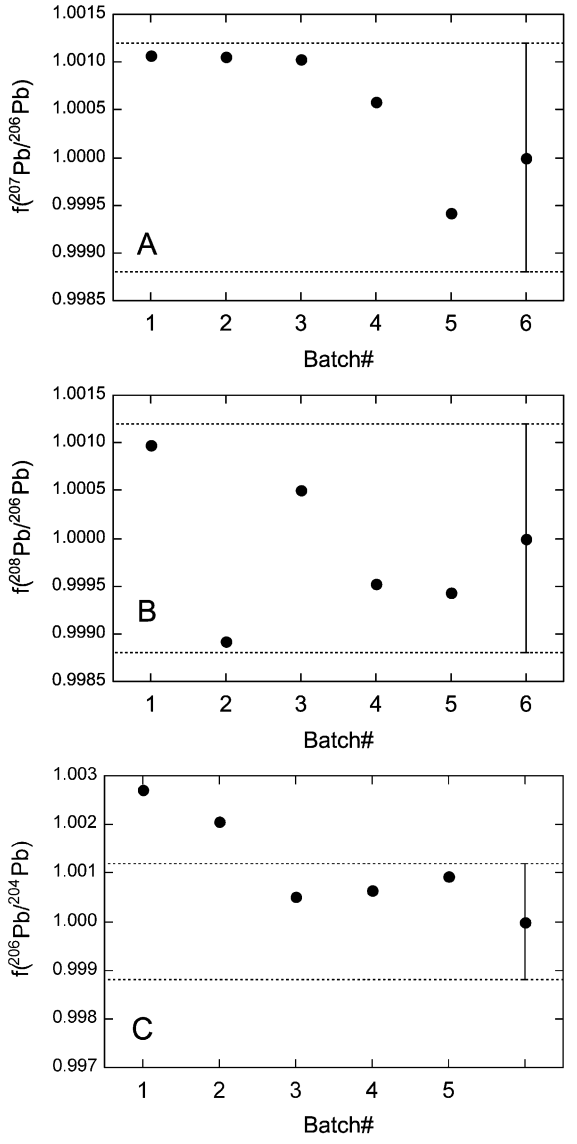

Fig. 8. Comparison of Pb-isotope data obtained by TIMS versus MC-ICP-MS at UQ. Datapoints represent projectiles from five different batches of Norma® bullets. Agreement is found within ca. 1.2 per mil in $^{207}Pb/^{206}Pb$ (panel A) and $^{208}Pb/^{206}Pb$. Difference in ratio expressed as the product between the TIMS and MC-ICP-MS values. The expected ratio of unity is shown along the right margin with 1.2 per mil coincidence limit shown as stippled lines. In $^{206}Pb/^{204}Pb$ (panel C), two datapoints plot outside the estimated reproducibility of 1.2 per mil.

pressure teflon vessels. Pb was purified with standard HBr–HCl anion-exchange resin technique. Results are given in Table 1 and illustrated in Fig. 9. Our isotope measurements for BCR-2 agree individually and as a mean with those of Woodhead and Hergt (2000), both in $^{208}Pb/^{204}Pb$ vs. $^{206}Pb/^{204}Pb$ and $^{207}Pb/^{204}Pb$ vs. $^{206}Pb/^{204}Pb$ space. In contrast to Woodhead and Hergt (2000), our two determinations for BHVO-2 were reproducible. The mean of our data is clearly different from the mean of that study (see Fig. 9), both in $^{206}Pb/^{204}Pb$ and $^{207}Pb/^{204}Pb$ vs. $^{206}Pb/^{204}Pb$ space. However, the variations in Pb-isotope composition of BHVO-2 determined by Woodhead and Hergt (2000) clearly exceed those of all the other USGS standards and the spread seen in their data is larger than the difference between their average and ours. Importantly, that variation cannot be explained by mass bias or mass 204 error but must, at least to some extent, be a true feature of the standard. It appears that our batch of BHVO-2 has a somewhat

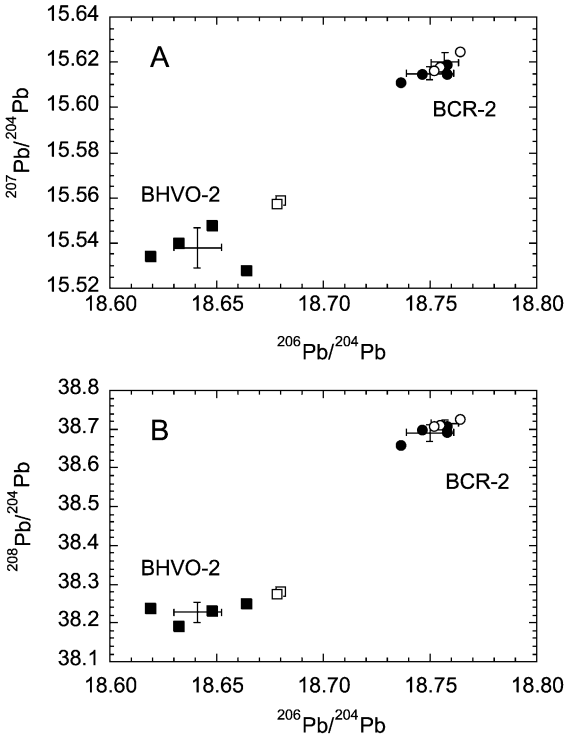

Fig. 9. Comparison of USGS standard compositions determined by MC-ICP-MS (open symbols) and double-spike TIMS technique (solid symbols; data from Woodhead and Hergt, 2000). Plotted are data of individual digestions and averages (as 1 sigma error bars). Excellent agreement was obtained for standard BCR-2 (circles), but BHVO-2 (squares) is much less reproducible (as seen, particularly, in the dataset of Woodhead and Hergt, 2000).

different isotope composition again, thereby rendering BHVO-2 virtually useless as an international isotopic standard. Incidentally, of all the USGS standards used in the UQ trace element laboratory, BHVO-2 shows by far the worst reproducibility for Pb concentration (Alan Greig, personal communication, 2001). That observation (i.e., reproducibility of 10% compared to 1–2% in other comparable rock standards) implies contamination most probably caused in the attempt at homogenising the standards. The 'nugget' effect (i.e., standard batches with unusually high Pb contents) could also explain the poor reproducibility of Pb-isotope ratios. Regardless, the excellent coincidence of our results for BCR-2 with those of Woodhead and Hergt (2000) show that MC-ICP-MS technology can reproduce the accuracy of double-spike TIMS data.

In view of the paucity of isotopically homogenous and well-characterised natural samples and rock standards (see above), we decided to further test the accuracy of our method with isochrons. A statistically well-defined isochron (preferably on U–Pb zircon dated material) is presently the best demonstration of accuracy and validity of high-precision Pb-isotope analytical methods. It has the further advantage of testing the method over a geologically adequate dynamic range. In the following, we present three datasets from samples of increasing matrix complexity (carbonate, silicate, and mixed sulphide).

5.3. Carbonate isochron

Moorbath et al. (1987) reported the first successful attempt at directly dating early diagenesis of microbial carbonate using Pb–Pb chronology. Their interpreted Pb–Pb age of 2839 ± 33 Ma fits well with correlative stratigraphy of Zimbabwean greenstone belts, as discussed by Dodson et al. (2001). For this study, we used the uneven numbered fragments (5 through to 23) of the original core (no. 2) drilled into the Mushandike limestone (samples courtesy of S. Moorbath). Carbonate fractions of ca. 200 mg samples were carefully dissolved in acetic acid at room temperature and Pb was purified by double-pass standard HBr–HCl anion-exchange technique. Silicate fractions were discarded. Pb-isotope data are reported in Table 1 and illustrated on Fig. 10. All isochron calculations were performed with Isoplot/Ex rev. 2.49 (Ludwig, 1999) always

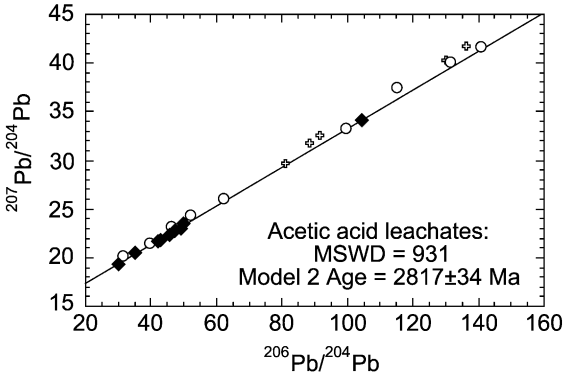

Fig. 10. Comparison of Pb-isotope data for Mushandike stromatolite subsamples from original drill core #2. Acetic acid leachates (solid diamond symbols) from this study were measured by MC-ICP-MS and yielded a model 2 age of 2817 ± 34 Ma. Moorbath et al. (1987) leached their samples with stronger acid (3 M HCl). Their leachates (open circles) define an indistinguishable model 2 age of 2826 ± 53 Ma. HCl-insoluble residues of Moorbath et al. (1987) are shown as open cross symbols. There is evidently a trend of increasing initial $^{207}Pb/^{206}Pb$, in which the gently leached carbonate fraction plots at the lower end, the 3 M HCl leached carbonate plots central in the array and the silicate fraction displays the highest apparent initial U/Pb.

using external reproducibility as the error except for analyses for which internal error was larger. Our acetic acid leachates define a linear data array that yields a model 2 regression age of 2817 ± 34 Ma (MSWD = 931). This age is well within error of Moorbath et al.'s (1987) original regression line of 2839 ± 33 Ma that was calculated using leachates, total dissolutions, and HCl-insoluble silicate residues. Even better coincidence is found if an age is calculated from Moorbath et al.'s (1987) leachates only, which yield a model 2 regression corresponding to an age of 2826 ± 53 Ma (MSWD = 369). Our principle conclusions are that we can reproduce a Pb–Pb regression age of natural samples and that the error of these particular regression lines reflects geological scatter. In other words, the scatter about Moorbath et al.'s (1987) regression line is not analytical artefact but a real feature of these samples. This contrasts with the observations of Woodhead and Hergt (1997) who found that double-spike corrected data yielded more precise regression dates for their carbonate samples. However, this largely reflects the much reduced dynamic range of their datasets compared to that of the Mushandike limestone.

An interesting detail of the Mushandike dataset is the apparent slight difference in initial isotope composition between the carbonate- and silicate-hosted Pb. The silicate fractions plot at the high $^{207}Pb/^{206}Pb$ limit of the array (Fig. 10) while our acetic acid leachates are at the lower $^{207}Pb/^{206}Pb$ limit. Moorbath et al.'s (1987) leachates with stronger acid (3 M HCl) plot central to the other two datasets. A more detailed discussion of these results will be presented elsewhere in combination with Sr-isotope and trace element data.

5.4. Metamorphic mineral isochron

Before attempting to measure very radiogenic Pb of natural samples, we successfully measured the isotope composition of NIST SRM 983 (see Table 1). NIST SRM 983 is not a widely used standard but its isotope composition is relatively well-known from work by U–Th–Pb geochronology specialists. As can be seen from Table 1, the average of five isotope ratio measurements of 12 ng NIST SRM 983, obtained over several days interspersed with other standard analyses, agrees well with the values of the MIT geochronology laboratory (S. Bowring, personal communication, 2000). This agreement is testimony to the low blank of the chemistry and MC-ICP-MS laboratory and underscores the fact that on-peak-zero measurements and ^{204}Hg-interference correction are robust, even for very small ^{204}Pb ion currents. However, for radiogenic Pb-isotope work, it is essential to achieve a very stable on-peak-zero baseline. We routinely test our purified Pb samples for expected ion yields with a defocussed beam and record relative intensities of masses 206 and 204. This allows us to identify the most radiogenic samples so that extra care can be taken with washout.

In order to minimise the likelihood of scatter in initial isotope ratio, metamorphic minerals (hornblende, plagioclase, sphene, and apatite) were separated for dating from a single 500 g sample of an early Archaean amphibolite (courtesy of S. Moorbath) from a tonalite gneiss region south of the Isua greenstone belt (for a geological overview, see Nutman et al., 1999). Mineral separates of plagioclase, sphene (2 ×) and apatite were prepared and a whole rock aliquot was powdered. Results for leached feldspar, whole rock, apatite, and two sphene fractions are reported in Table 1 and illustrated on Fig. 11. The first observation is the excellent colinearity ($r^2 = 0.9999998$) of the datapoints. The five-point regression line yields a model 1 (assuming only analytical scatter) age of 3129.6 ± 4.9 Ma and model 2 (assuming geological scatter) age of 3131.4 ± 2.4 Ma. This observation indicates that coherent MC-ICP-MS Pb-isotope data can be obtained over a wide dynamic range ($^{206}Pb/^{204}Pb$ varies from 12.05 to 575). The wide range in $^{205}Tl/^{204}Pb$ from ca. 5 to >100 appears to have no adverse effect on our ability to measure the $^{206}Pb/^{204}Pb$ ratio.

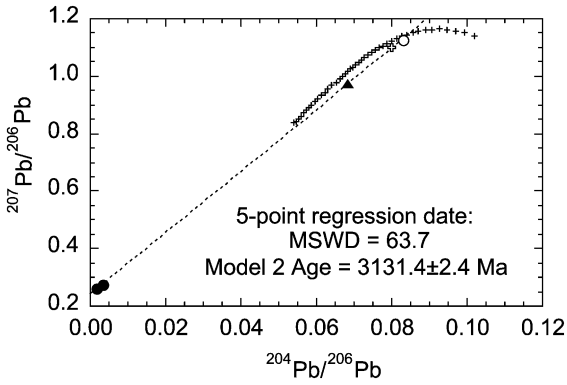

Fig. 11. Pb-isotope compositions of metamorphic minerals of an early Archaean amphibolite from West Greenland shown in a Tera-Wasserburg diagram. Two sphene fractions are shown as solid circles, plagioclase as open circle, whole rock as open cross, and apatite as solid triangle. Symbol sizes exceed error bars. Regressions calculated with an error correlation of 0.95, to which the regression parameters are insensitive. The mantle evolution line (small + symbols) of Kramers and Tolstikhin (1997) is intersected at ca. 3.4 Ga by the five-point regression line (dotted line), yielding a model 2 age of 3131.4 ± 2.4 Ma.

Nevertheless, despite the excellent colinearity and the very small degree of geological scatter (as evidenced by the very small regression error) the high MSWD (63.7) of the regression still indicates a probability of zero for the calculated age. Thus, although the excellent co-linearity is encouraging, the high MSWD shows that the regression results do not pass as the ultimate test for the validity of our method.

Regression of the plagioclase and sphene datapoints alone lowers the MSWD to 3.44 but yields unchanged three-point ages of 3130 ± 4.8 Ma (model 1) and 3132 ± 15 Ma (model 2). However, even that regression line would not qualify as a true isochron. Individual two-point ages calculated with plagioclase

and the two sphene fractions are also identical to the multi-point regression dates (3129.2 ± 0.4 and 3131.6 ± 2.0 Ma, respectively). Therefore, despite the high MSWD, the obtained age information appears to be very robust, as the estimated dates only range narrowly from 3129.2 to 3132.0 Ma. We believe that the small scatter (albeit outside analytical uncertainty) about the regression line is real and reflects the imperfection of natural rocks/minerals, such as incomplete isotope equilibrium during metamorphic recrystallisation. For routine dating purpose by accurate and precise Pb-isotope techniques (Tl-normalised MC-ICP-MS and double/triple-spike) it will be necessary to define new probability parameters. Pb–Pb chronology has thus reached the same dilemma as U–Pb zircon and Ar–Ar geochronology in that most natural materials show scatter in excess of significantly improved experimental accuracy.

5.5. Sulphide mineral isochron

The Great Dyke of Zimbabwe offers a good chance of yielding a precise, true Pb–Pb isochron as it is isotopically very homogenous. Mukasa et al. (1998) obtained concordant Sm–Nd and Pb–Pb whole rock/mineral isochrons of 2572 ± 43 and 2596 ± 14 Ma, despite their samples having been taken from outcrops several hundred kilometers apart. A number of U–Pb mineral age determinations for the Great Dyke and its satellites exist. Mukasa et al. (1998) reported a 2587 ± 8 Ma U–Pb age for rutiles. However, because the rutile data are reversely discordant, both Wingate (2000) and Armstrong and Wilson (2000) proposed that the weighted mean Pb–Pb age of 2575 ± 5 Ma represented a better age estimate. Wingate's (2000) own 2581 ± 11 Ma U–Pb zircon age for a gabbro of the Darwendale subchamber is, within error, identical to both the U–Pb and Pb–Pb ages of the rutiles dated by Mukasa et al. (1998). Armstrong and Wilson (2000) obtained an identical but more precise age of 2579 ± 3 Ma for zircons extracted from a websterite of the Great Dyke itself, while a structurally younger granitoid dyke yielded a U–Pb zircon age of 2574 ± 7 Ma. The mean age from those three independent age determinations on four different samples is 2577.6 ± 2.3 Ma (using the weighted Pb–Pb age of 2575 ± 5 Ma for the rutiles analysed by Mukasa et al., 1998). Wingate (2000) also reported Pb–Pb ages of baddeleyites from the Great Dyke and a satellite dyke for which he obtained a combined age of 2574 ± 2 Ma. At the quoted precision, the baddeleyite age is slightly younger than the zircon ages. However, the very high precision of the baddeleyite age estimate assumes correctness of the underlying statistical data treatment (in this case, maximum-likelihood mixture modelling) and for this paper, we prefer to compare our data with the U–Pb zircon results.

For this study, a mixed sulphide mineral concentrate (pyrrhotite, pentlandite, chalcopyrite with oxide mineral inclusions, including rutile) from the Main Sulphide Zone of the Great Dyke (e.g., Oberthür et al., 1997) was dissolved in four successive steps (1 h in 1 M HBr at 20 °C, 1 h in 3 M HBr at 20 °C, 3 h in aqua regia at 80 °C, 12 h in aqua regia at 120 °C) all of which were treated as individual samples (similar to the step-wise leaching procedure of Frei and Kamber, 1995). Data are reported in Table 1 and Fig. 12. The successive leaching steps released increasingly radiogenic Pb (possibly from oxide inclusions) which define a Pb–Pb isochron (MSWD = 0.63) age of 2578.3 ± 0.9 Ma. The much less radiogenic whole rock and silicate mineral datapoints by Mukasa et al. (1998) plot exactly along the sulphide isochron (Fig.

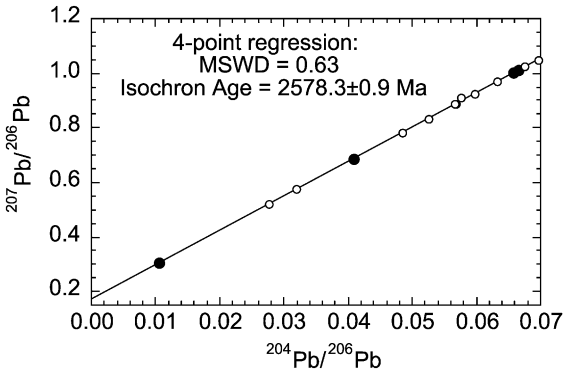

Fig. 12. Pb-isotope compositions of progressively dissolved magmatic sulphide concentrate (four solid circles) from the Main Sulphide Zone, Great Dyke, shown in a Tera-Wasserburg diagram. Symbol sizes exceed error bars. Regression calculated with an error correlation of 0.95, to which the regression parameters are insensitive, yields an isochron (MSWD = 0.63) age of 2578.3 ± 0.9 Ma. Great Dyke whole rock and silicate mineral data of Mukasa et al. (1998) shown for comparison (small open circles).

12). The sulphide datapoints are also very well aligned ($r^2 = 0.998$) in thorogenic Pb-isotope space. We interpret these lines to indicate mixture between unradiogenic (sulphide) and radiogenic (possibly microscopic oxide inclusions) components from an undisturbed sulphide horizon with no discernible initial Pb-isotope heterogeneity. Such mixing lines contain valid age information (e.g., Frei et al., 1997). The isochron age of 2578.3 ± 0.9 Ma is identical to the mean 2577.6 ± 2.3 Ma U–Pb zircon age for the Great Dyke. Note that all the reported age errors do not include uncertainties of decay constants, which is permissible for the comparison of relative ages. The coincidence in age clearly demonstrates that our Pb analytical technique is valid and can successfully be applied to natural samples.

It is worth noting that in practice, binary mixing lines both of natural origin or purposefully created in the laboratory are potentially the best materials to test accuracy of MC-ICP-MS and double- and triple-spike methods. This is because perfect co-linearity can indeed be expected.

6. Summary

We present an extensive set of standard Pb-isotope data as well as a series of data from natural samples to show that reproducible and accurate Pb-isotope ratios can be obtained by Tl-doped MC-ICP-MS technique over a wide dynamic range of geological interest. Mass discrimination behaviour of Pb and Tl was studied in detail and it was found that within error, the mass discrimination slopes can be corrected using the exponential or power-law. There exists no physical rationale for 'optimising' the Tl normalisation ratio (as suggested by Rehkämper and Mezger, 2000), nor is there a need to adjust the Tl fractionation coefficient (as suggested by White et al., 2000). When all our NIST SRM 981 data are normalised with $^{205}Tl/^{203}Tl$ of 2.38869 the following averages and reproducibilities were obtained: $^{207}Pb/^{206}Pb = 0.91461 \pm 18$; $^{208}Pb/^{206}Pb = 2.1674 \pm 7$; and $^{206}Pb/^{204}Pb = 16.941 \pm 6$ (Table 1). The quoted two sigma standard deviations of the mean correspond to 149, 330, and 374 ppm, respectively. Accuracies are well within uncertainties of the Galer and Abouchami (1998) and Thirlwall (2000a) reference values. The largest component of the uncertainties stems from the Pb data alone and is not caused by differential behaviour of Pb and Tl. Better reproducibilities could be obtained with longer ion acquisition but in routine operation the presently achieved reproducibility is already exposing natural isotopic variation in excess of analytical scatter. Careful operation of MC-ICP-MS enables production of high quality data not only for standards but also for natural samples.

Acknowledgements

The UQ MC-ICP-MS was purchased with partial support from an ARC equipment grant to KDC. Nippon Oil Exploration Limited, Japan National Oil Corporation and Japan Energy Development Company Limited are thanked for their continued financial support of ACQUIRE through commercial contracts. Alan Greig, Immo Wendb, Yaoling Niu and Huaikun Li are thanked for technical input. Stephen Moorbath (Oxford) and Thomas Oberthür (Hannover) generously provided samples. Reviews by S. Galer and M. Thirlwall helped to improve the manuscript. **[RR]**

References

Armstrong, R., Wilson, A.H., 2000. A SHRIMP U–Pb study of zircons from the layered sequence of the Great Dyke, Zimbabwe, and a granitoid anatectic dyke. Earth Planet. Sci. Lett. 180, 1–12.

Belshaw, N.S., Freedman, P.A., O'Nions, R.K., Frank, M., Guo, Y., 1998. A new variable dispersion double-focusing plasma mass spectrometer with performance illustrated for Pb isotopes. Int. J. Mass Spectrom. 181, 51–58.

Collerson, K.D., 1995. Developments in radiogenic isotope geochemistry at The University of Queensland: geochronological and geochemical applications. In: Johnson, R.W., King, C.R. (Eds.), Queensland: The State of Science Proceedings, Brisbane, 15–16 July 1994. R. Soc. Queensl., pp. 305–337.

Dodson, M.H., Williams, I.S., Kramers, J.D., 2001. The Mushandike granite: further evidence for 3.4 Ga magmatism in the Zimbabwe craton. Geol. Mag. 138, 31–38.

Frei, R., Kamber, B.S., 1995. Single mineral Pb–Pb dating. Earth Planet. Sci. Lett. 129, 261–268.

Frei, R., Villa, I.M., Nägler, T.F., Kramers, J.D., Przybylowicz, W.J., Prozesky, V.M., Hofmann, B.A., Kamber, B.S., 1997. Single mineral dating by the Pb–Pb step-leaching method; assessing the mechanisms. Geochim. Cosmochim. Acta 61, 393–414.

Galer, S.J.G., Abouchami, W., 1998. Practical application of lead

triple spiking for correction of instrumental mass discrimination. Mineral. Mag. 62A, 491–492.

Hirata, T., 1996. Lead isotope analysis of NIST standard reference materials using multiple collector-inductively coupled plasma mass spectrometry coupled with modified external correction method for mass discrimination effect. Analyst 121, 1407–1411.

Kramers, J.D., Tolstikhin, I.N., 1997. Two terrestrial lead isotope paradoxes, forward transport modelling, core formation and the history of the continental crust. Chem. Geol. 139, 75–110.

Ludwig, K.R., 1999. Isoplot/Ex rev. 2.49—a geochronological toolkit for Microsoft Excel. Berkeley Geochron. Center Spec. Publ. 1a, 1–52.

Maréchal, C.N., Télouk, P., Albarède, F., 1999. Precise analysis of copper and zinc isotopic compositions by plasma-source mass spectrometry. Chem. Geol. 156, 251–273.

Moorbath, S., Taylor, P.N., Orpen, J.L., Treloar, P., Wilson, J.F., 1987. First direct radiometric dating of Archaean stromatolitic limestone. Nature 326, 865–867.

Mukasa, S.B., Wilson, A.H., Carlson, R.W., 1998. A multi-element geochronologic study of the Great Dyke, Zimbabwe: significance of the robust and reset ages. Earth Planet. Sci. Lett. 164, 353–369.

Münker, C., Weyer, S., Mezger, K., Rehkämper, M., Wombacher, F., Bischoff, A., 2000. Nb-92-2r-92 and the early differentiation history of planetary bodies. Science 289, 1538–1542.

Nutman, A.P., Bennett, V.C., Friend, C.R.L., Norman, M.D., 1999. Meta-igneous (non-gneissic) tonalites and quartz-diorites from an extensive ca. 3800 Ma terrain south of the Isua supracrustal belt, southern West Greenland: constraints on early crust formation. Contrib. Mineral. Petrol. 137, 364–388.

Oberthür, T., Cabri, L.J., Weiser, T.W., McMahon, G., Müller, P., 1997. Pt, Pd and other trace elements in sulfides of the Main Sulfide Zone, Great Dyke, Zimbabwe: a reconnaissance study. Can. Mineral. 35, 597–609.

Rehkämper, M., Halliday, A.N., 1998. Accuracy and long-term reproducibility of lead isotopic measurements by multiple-collector inductively coupled plasma mass spectrometry using an external method for correction of mass discrimination. Int. J. Mass Spectrom. 181, 123–133.

Rehkämper, M., Mezger, K., 2000. Investigation of matrix effects for Pb isotope ratio measurements by multiple collector ICP-MS: verification and application of optimised analytical protocols. J. Anal. At. Spectrom. 15, 1451–1460.

Scherer, G., Münker, C., Mezger, K., 2001. Calibration of the lutetium-hafnium clock. Science 293, 683–687.

Schoenberg, R., Kamber, B., Collerson, K.D., Eugster, H., in press. New W-isotope evidence for rapid terrestrial accretion and very early core formation. Geochim. Cosmochim. Acta.

Thirlwall, M.F., 2000a. Inter-laboratory and other errors in Pb isotope analyses investigated using a $^{207}Pb-^{204}Pb$ double spike. Chem. Geol. 163, 299–322.

Thirlwall, M.F., 2000b. Precise Pb isotope analysis of standards and samples using an Isoprobe multicollector ICP-MS: comparisons with double spike thermal ionization data. J. Conf. Abstr. 5, 996.

Todt, W., Cliff, R.A., Hanser, A., Hofmann, A.W., 1996. Evaluation of a $^{202}Pb-^{205}Pb$ double spike for high-precision lead isotope analysis. In: Basu, A., Hart, S. (Eds.), Earth Processes: Reading The Isotopic Code. Geophys. Monogr. Am. Geophys. Union, Washington, pp. 429–437.

White, W.M., Albarède, F., Télouk, P., 2000. High-precision analysis of Pb isotope ratios by multi-collector ICP-MS. Chem. Geol. 167, 257–270.

Wingate, M.T.D., 2000. Ion microprobe U–Pb zircon and baddeleyite ages for the Great Dyke and its satellite dykes, Zimbabwe. S. Afr. J. Geol. 103, 74–80.

Woodhead, J.D., Hergt, J.M., 1997. Application of the 'double spike' technique to Pb-isotope geochronology. Chem. Geol. 138, 311–321.

Woodhead, J.D., Hergt, J.M., 2000. Pb-isotope analyses of USGS reference materials. Geostand. Newsl. 24 (06), 33–38.